

Quantum-interference-assisted photon blockade in a cavity via parametric interactions

Bijita Sarma* and Amarendra K. Sarma†

Department of Physics, Indian Institute of Technology Guwahati, Guwahati 781039, Assam, India

(Received 17 August 2017; published 13 November 2017)

We propose a scheme to achieve a strong photon antibunching with a degenerate optical parametric amplifier coupled to a cavity via unconventional photon blockade. The photon blockade occurs as a result of the suppression of two-photon excitation due to a quantum interference effect between different transition paths. Via analytical calculations, we find out the conditions for optimized photon antibunching in terms of parametric gain and the parametric amplifier pump phase. Calculations of second-order correlation function demonstrate strong photon antibunching. The numerical results are compared with the analytical results and both are in complete agreement. Under the optimal parameters, the system can be used to generate sub-Poissonian light.

DOI: [10.1103/PhysRevA.96.053827](https://doi.org/10.1103/PhysRevA.96.053827)

I. INTRODUCTION

Single-photon sources are necessary for possible applications of photons in quantum information processing and quantum communication. One of the ways of obtaining single photons is via the mechanism called photon blockade (PB). Using PB one can produce sub-Poissonian light from a cavity when driven by a classical light field. It is a quantum optical effect that arises as a result of the quantum anharmonicity ladder in a nonlinear cavity. It is named so, because the resonant injection of more photons into a nonlinear cavity mode is prevented when one photon is already present in it [1]. PB is observed through antibunching in photon correlation measurements. There have been several proposals for achieving single-photon blockade in coupled cavity arrays [2–4], one-dimensional optical waveguides [5], qubit-cavity coupled systems [6], optomechanical systems [7–10] and circuit-QED systems [11], and also multiphoton blockade in some setups [12–14]. In analogy to PB, there are proposals for phonon blockade also, in nanomechanical resonators [15–17]. On experimental fronts, PB has been observed by resonant laser excitation on a single trapped atom in a cavity [18], a single atom coupled to a microtoroidal cavity [19], a single quantum dot embedded in a strongly coupled cavity [20], and circuit-QED systems [21,22]. There are several proposals that are based on applications of PB which include a quantum-optical Josephson interferometer [23], fermionization of photons in an array of nonlinear cavities [24], and crystallization of polaritons in arrays of lossy nonlinear resonators [25].

The most striking constraint in realizing PB is that it requires a strong nonlinearity, either a Kerr nonlinearity of the cavity mode [1] or atom-cavity coupling [18], whose magnitude should well exceed the mode broadening. While working in the single-photon regime, a strong nonlinearity is not so easy to realize. However, in a recent work by Liew and Savona [26], a new mechanism was invoked to realize PB, based on quantum interference between excitation pathways that is referred to as unconventional photon blockade (UPB). It was shown that strong antibunching could be achieved with a weak Kerr nonlinearity in a system consisting of two

coupled polaritons. Realization of UPB has been predicted in a few systems, such as a coupled single quantum dot-cavity system [27], a lossy bimodal nanocavity where both the modes are coupled to a quantum dot [28,29], symmetric and antisymmetric modes in weakly nonlinear photonic molecules [30], coupled nonlinear photonic molecules [31], coupled single-mode cavities with third-order nonlinearities [32–36], coupled cavities with second-order nonlinearity [37,38], Gaussian squeezed states [39], and coupled optomechanical systems [40,41].

In this work, we study the possibility of realizing UPB in a cavity that includes a degenerate optical parametric amplifier (OPA). Introducing the OPA, one can create new paths for photon excitation that may lead to destructive quantum interference in the two-photon excitation pathway [42]. We find out the optimal conditions for achieving this. The validity of the optimal conditions is also confirmed via numerical simulations. We also analyze the effects of pure dephasing induced decoherence on the UPB.

The remainder of the paper is organized as follows. In Sec. II, we introduce a model to describe the system and derive the optimal conditions for strong antibunching. In Sec. III, we analyze photon antibunching by calculating the equal-time second-order correlation function numerically using the optimal conditions and compare it with the analytical results. Finally we summarize our results in Sec. IV.

II. THEORY

We consider a system consisting of a degenerate OPA inside a Fabry-Perot cavity. The setup under consideration can be modeled schematically as shown in Fig. 1(a). The Hamiltonian for the system can be written as [42]

$$H_0 = \omega_a a^\dagger a + iG(e^{i\theta} a^{\dagger 2} - e^{-i\theta} a^2) + \Omega(a^\dagger e^{i\omega_l t} + a e^{-i\omega_l t}), \quad (1)$$

where a (a^\dagger) is the annihilation (creation) operator for the optical mode, ω_a is the resonance frequency of the cavity field, and ω_l is the driving laser frequency. Here, Ω is the driving laser amplitude, G is the nonlinear gain of the OPA which is proportional to the amplitude of the pump field driving the OPA, and θ is the phase of the field driving the OPA.

*s.bijita@iitg.ernet.in

†aksarma@iitg.ernet.in

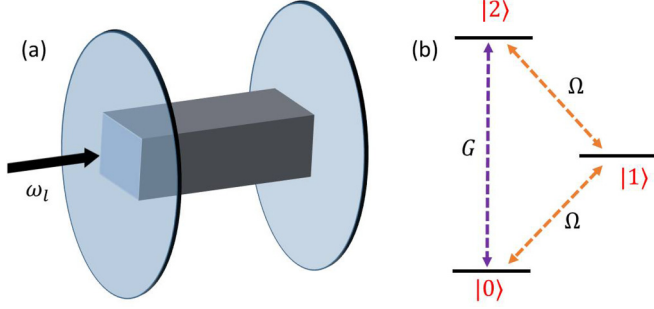


FIG. 1. (a) Schematic diagram of the cavity setup with an OPA which is pumped by a laser (not shown here) to produce parametric amplification in the cavity. (b) Transition paths of the system for quantum interference. There are two paths leading to two-photon excitation: from $|0\rangle$ to $|1\rangle$ and then $|1\rangle$ to $|2\rangle$, excited by the driving field; and the direct transition from $|0\rangle$ to $|2\rangle$ due to the OPA. Quantum interference can occur between these two paths.

In a rotating frame, the Hamiltonian is transformed to

$$H = \Delta_a a^\dagger a + iG(e^{i\theta} a^{\dagger 2} - e^{-i\theta} a^2) + \Omega(a^\dagger + a), \quad (2)$$

where $\Delta_a = \omega_a - \omega_l$ is the cavity-light detuning. The effect of the OPA coupling, G , is usually to produce some change in the cavity frequency of the system. The eigenstates of the OPA Hamiltonian, i.e., Eq. (1) with $\Omega = 0$, are squeezed number states, given by $S(\xi)|n_a\rangle$, where $S(\xi) = e^{\xi(e^{i\theta} a^{\dagger 2} - e^{-i\theta} a^2)}$, with $\xi = \frac{1}{2} \tanh^{-1}(\frac{2G}{\omega_a})$ (see Appendix). In this case the eigenvalues are given by $E_{n_a} = \omega_a(n_a \cosh 2\xi + \sinh^2 \xi) - G(2n_a + 1) \sinh 2\xi$. For $G \ll \omega_a$, it can preferably be assumed that $E_{n_a} \approx \omega_a n_a$. Also, assuming a weak driving condition, i.e., $\Omega \ll \kappa$, where κ is the cavity decay rate, the photon number Hilbert space can be truncated to low values. Therefore, under these assumptions, we truncate the states according to $n \leq 2$, where $|n\rangle$ is the photon number Fock-state basis [31]:

$$|\psi\rangle = C_0|0\rangle + C_1|1\rangle + C_2|2\rangle, \quad (3)$$

where C_n 's are the amplitudes of the quantum states for which the corresponding occupation probability is given by $|C_n|^2$. The values of the coefficients C_n can be obtained by solving the Schrödinger equation, also taking into account the dissipations in the system:

$$i \frac{d|\psi\rangle}{dt} = H'|\psi\rangle, \quad (4)$$

where H' is the effective non-Hermitian Hamiltonian:

$$H' = \Delta'_a a^\dagger a + iG(e^{i\theta} a^{\dagger 2} - e^{-i\theta} a^2) + \Omega(a^\dagger + a) \quad (5)$$

with $\Delta'_a = \Delta_a - i\kappa/2$. Substituting the state $|\psi\rangle$ and Hamiltonian H' into the Schrödinger equation $i \frac{d|\psi\rangle}{dt} = H'|\psi\rangle$, we obtain a set of equations for the coefficients:

$$\begin{aligned} i \frac{\partial C_0}{\partial t} &= \Omega C_1 - i\sqrt{2}G e^{-i\theta} C_2, \\ i \frac{\partial C_1}{\partial t} &= \Omega C_0 + \Delta'_a C_1 + \sqrt{2}\Omega C_2, \\ i \frac{\partial C_2}{\partial t} &= i\sqrt{2}G e^{i\theta} C_0 + \sqrt{2}\Omega C_1 + 2\Delta'_a C_2. \end{aligned} \quad (6)$$

The steady-state solution can be found by solving the coupled equations for the coefficients. For complete PB, the probability of a photon in state $|C_2\rangle$ equals zero when the optimal condition is satisfied. Therefore, we consider $C_2 = 0$ in Eqs. (6) for PB. Under the weak driving condition, the first equation in Eqs. (6) is always approximatively satisfied. Therefore, we only consider the last two equations for further calculations:

$$\begin{aligned} \Omega C_0 + \Delta'_a C_1 &= 0, \\ iG e^{i\theta} C_0 + \Omega C_1 &= 0. \end{aligned} \quad (7)$$

It should be noted that in absence of the OPA, i.e., for $G = 0$, one cannot find any nontrivial solution from Eqs. (7). After finding out the necessary and sufficient conditions for these equations to have a solution, more simplifications lead us to the following optimum conditions:

$$\begin{aligned} G_{\text{opt}} &= 2\Omega^2 / \sqrt{\kappa^2 + 4\Delta_a^2}, \\ \theta_{\text{opt}} &= \arctan\left(-\frac{2\Delta_a}{\kappa}\right). \end{aligned} \quad (8)$$

Interestingly, these conditions depend on the cavity-detuning, driving laser amplitude and the cavity linewidth. Since the optimal conditions correspond to the parameters of the pump field driving the OPA, these are expected to be controlled by tuning the OPA pump field. In passing, it may be worthwhile to mention that the approximate analytical model developed here was originally formulated by Bamba *et al.* [31], which again was motivated by the numerical work of Liew and Savona [26]. Liew and Savona discussed the strong photon antibunching effect in a pair of coupled quantum boxes by solving the quantum master equation numerically. In the next section, we solve the quantum master equation numerically using the analytical optimum conditions, and find that numerical results are in conformity with the approximate analytical model.

III. RESULTS AND DISCUSSIONS

The realization of PB can be analyzed by the normalized zero-time-delay second-order correlation function given by

$$g^{(2)}(0) = \frac{\langle a^\dagger(t)a^\dagger(t)a(t)a(t) \rangle}{\langle a^\dagger(t)a(t) \rangle^2}. \quad (9)$$

This quantity characterizes the joint probability of detecting two photons at the same time. For PB, we have assumed that the cavity is driven by a weak classical field. The master equation of the density operator ρ for the driven system reads as

$$\dot{\rho} = i[\rho, H] + L_a(\rho), \quad (10)$$

where $L_a(\rho) = \frac{\kappa}{2}(2\rho a^\dagger - a^\dagger \rho - \rho a)$ is the Liouvillian operator for the optical mode. The steady-state value of $g^{(2)}(0)$ can be found numerically by solving the master equation and from the steady-state density matrix operator as

$$g^{(2)}(0) = \frac{\text{Tr}(\rho a^\dagger a^\dagger a a)}{[\text{Tr}(\rho a^\dagger a)]^2}. \quad (11)$$

Here, the quantum interference effect with different transition paths occurs as shown in Fig. 1(b). The quantum interference can happen between the two paths: from $|0\rangle$ to

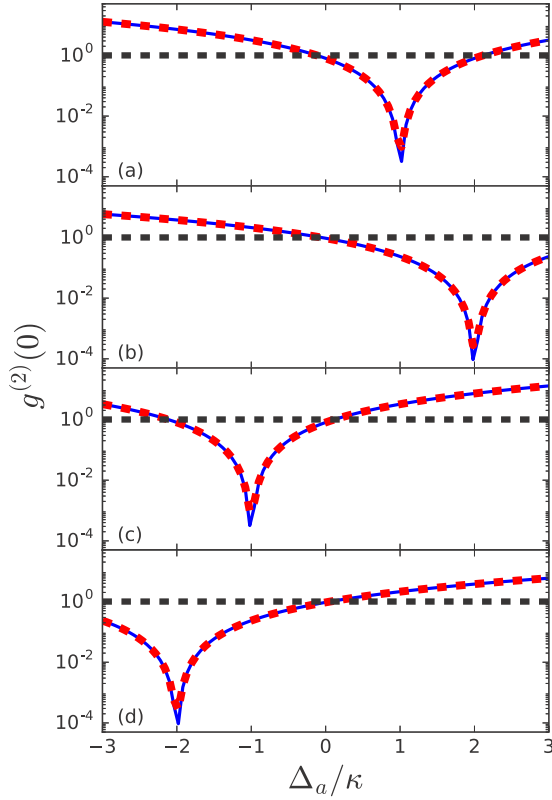


FIG. 2. Numerical (red dots) and analytical (blue line) results for the zero-time-delay second-order correlation function, $g^{(2)}(0)$, as a function of normalized detuning Δ_a/κ . OPA parameters are $G/\kappa = 8.94 \times 10^{-5}$, $\theta/\pi = -0.352$ in (a), $G/\kappa = 4.85 \times 10^{-5}$, $\theta/\pi = -0.422$ in (b), $G/\kappa = 8.94 \times 10^{-5}$, $\theta/\pi = 0.352$ in (c), and $G/\kappa = 4.85 \times 10^{-5}$, $\theta/\pi = 0.422$ in (d).

$|1\rangle$ and then $|1\rangle$ to $|2\rangle$, excited by the driven field; and the direct transition $|0\rangle$ to $|2\rangle$ assisted by the OPA.

A. Numerical solution

For all the calculations in this paper, we have considered $\Omega/\kappa = 0.01$ for weak driving condition. In Fig. 2, we have discussed the variation of the second-order correlation function at zero-time delay, $g^{(2)}(0)$, for different optimum values calculated according to Eq. (8). $g^{(2)}(0)$ is plotted as a function of normalized detuning Δ_a/κ for optimal values of G and θ . The red dots show the numerical simulation results. In Figs. 2(a) and 2(b), values of G and θ are considered to satisfy Eq. (8) for the corresponding value of Δ_a in the red-detuned region. In Fig. 2(a), the optimized values are $G_{\text{opt}} = 8.94 \times 10^{-5}\kappa$ and $\theta_{\text{opt}} = -0.352\pi$ that correspond to the optimum values for $\Delta_a/\kappa = 1$. As expected, $g^{(2)}(0)$ shows a strong antibunching effect at an exact value of $\Delta_a/\kappa = 1$, as precisely predicted by the optimal parameters calculated analytically. In Fig. 2(b), optimized values are $G/\kappa = 4.85 \times 10^{-5}$, $\theta/\pi = -0.422$ for $\Delta_a/\kappa = 2$. In this case also, $g^{(2)}(0)$ shows a strong antibunching effect at an exact value of $\Delta_a/\kappa = 2$. In both these cases there is no antibunching observed in the blue-detuning regime. For Figs. 2(c) and 2(d), G and θ values are considered to satisfy the optimal parameter calculations for Δ_a in the blue-detuning regime. In Figs. 2(c)

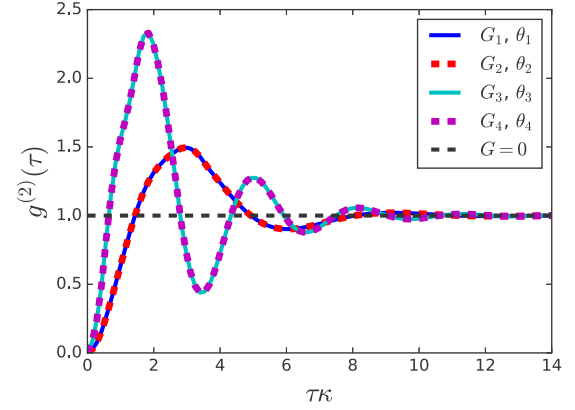


FIG. 3. Time evolution of the second-order correlation function, $g^{(2)}(\tau)$. The OPA parameters are $G_1 = 8.94 \times 10^{-5}\kappa$, $\theta_1 = -0.352\pi$, $G_2 = 4.85 \times 10^{-5}\kappa$, $\theta_2 = -0.422\pi$, $G_3 = 8.94 \times 10^{-5}\kappa$, $\theta_3 = 0.352\pi$, and $G_4 = 4.85 \times 10^{-5}\kappa$, $\theta_4 = 0.422\pi$.

and 2(d), optimum values are considered for $\Delta_a/\kappa = -1$ and -2 , respectively. Here, $G_{\text{opt}} = 8.94 \times 10^{-5}\kappa$ and $\theta_{\text{opt}} = 0.352\pi$ in Fig. 2(c) and $G/\kappa = 4.85 \times 10^{-5}$, $\theta/\pi = 0.422$ in Fig. 2(d). Again, a strong antibunching is observed at $\Delta_a/\kappa = -1$ and -2 , respectively, as predicted by the optimal conditions. Therefore, the simulation results obtained by the solving master equation verify the optimized conditions in Eq. (8) precisely.

An analytical expression for $g^{(2)}(0)$ in terms of the probabilistic coefficients can also be derived. The second-order degree of coherence can be written as

$$g^{(2)}(0) = \frac{2|C_2|^2}{(|C_1|^2)^2}. \quad (12)$$

In the weak-pumping limit, the ground-state population can be assumed to be unity and the population in other levels can be considered to be negligible. In that case, we may assume that $C_0 \approx 1$. Then Eqs. (7) transform to

$$\begin{aligned} \Omega + \Delta'_a C_1 + \sqrt{2}\Omega C_2 &= 0, \\ i\sqrt{2}G e^{i\theta} + \sqrt{2}\Omega C_1 + 2\Delta'_a C_2 &= 0. \end{aligned} \quad (13)$$

Hence, the coefficients to be used for the calculation of $g^{(2)}(0)$ are obtained as

$$\begin{aligned} C_1 &= \frac{\Omega(iG e^{i\theta} - \Delta'_a)}{\Delta_a'^2 - \Omega^2}, \\ C_2 &= -\frac{\Delta'_a C_1 + \Omega}{\sqrt{2}\Omega}. \end{aligned} \quad (14)$$

Now we can compare the analytical results with the numerical simulation results. The blue lines in Figs. 2(a)–2(d) correspond to the analytical results. The analytical results are in complete conformity with the numerical results. The black, dashed line in Fig. 2 represents both the numerical and analytical results for the $G = 0$ case, i.e., without the insertion of the OPA medium in the cavity. We can see that without the OPA medium, no antibunching is observed. Therefore by using the OPA interactions, a strong antibunching with sub-Poissonian quantum statistics for cavity field output can be achieved.

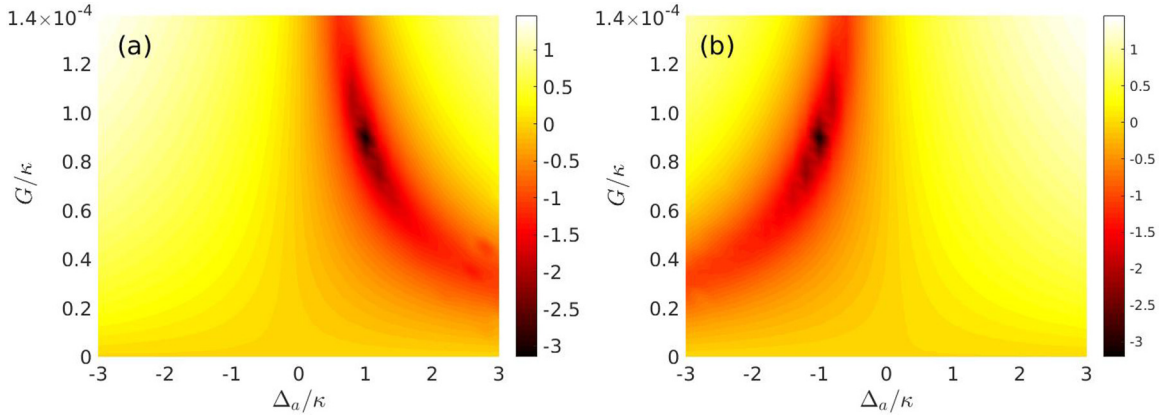


FIG. 4. Numerical results for the zero-time-delay second-order correlation function, $g^{(2)}(0)$, as a function of normalized detuning Δ_a/κ . Other parameters are $\Omega/\kappa = 0.01$. In (a) $\theta/\pi = -0.352$ and in (b) $\theta/\pi = 0.352$.

Figure 3 shows the time evolution of the second-order correlation function $g^{(2)}(\tau)$ that is calculated as

$$g^{(2)}(\tau) = \frac{\langle a^\dagger(t)a^\dagger(t+\tau)a(t+\tau)a(t) \rangle}{\langle a^\dagger(t)a(t) \rangle^2}. \quad (15)$$

$g^{(2)}(\tau)$ is proportional to the joint probability of detecting one photon at time $t = \tau$, provided another photon was detected at time $t = 0$, at that position [43]. The plots show $g^{(2)}(\tau)$ for different optimal conditions. We can observe that at $\tau = 0$, $g^{(2)}(0) = 0$ and for other delay times $g^{(2)}(\tau) > g^{(2)}(0)$. Therefore, it clearly demonstrates that the emitted photons are antibunched and sub-Poissonian in nature.

To further investigate the antibunching effects, we calculated $g^{(2)}(0)$ as a function of cavity-light detuning Δ_a/κ and OPA gain G/κ with optimized values of θ . In Fig. 4(a), phase is assumed to be -0.352π , which corresponds to the optimum value for $\Delta_a/\kappa = 1$. As expected, a strong PB occurs near the red detuning with $\Delta_a \approx \kappa$, and it occurs at $G/\kappa \approx 8.94 \times 10^{-5}$ as optimized precisely in Eq. (8). However, for the blue-detuned regime with $\Delta_a \approx -\kappa$, there is no strong antibunching because the phase of $\theta = -0.352\pi$ is not an optimized value in this case. In Fig. 4(b), $\theta/\pi = 0.352$ corresponds to $\Delta_a/\kappa = -1$. Here also, a strong antibunching occurs near the blue-detuned regime with $\Delta_a \approx -\kappa$ again at $G/\kappa \approx 8.94 \times 10^{-5}$; whereas, there is no PB in the red-detuning regime in this case. It is to be noted that, since G_{opt} expression is quadratic in Δ_a , for red and blue detuning, the G_{opt} value does not change. But the optimum value of OPA pump phase is different in these two regimes.

Figure 5 illustrates the variation of $g^{(2)}(0)$ as a function of cavity-light detuning Δ_a/κ and OPA pump phase θ with an optimized coupling strength $G/\kappa = 8.94 \times 10^{-5}$. A red-blue detuning asymmetric feature for $g^{(2)}(0)$ is observed, which is related to the OPA phase θ . For $\Delta_a \approx \kappa$ in the red-detuning regime, $g^{(2)}(0)$ exhibits a strong sub-Poissonian quantum statistics at a phase of $\theta/\pi \approx -0.35$. For this θ value, $g^{(2)}(0)$ does not show any antibunching in the blue-detuning regime. Similar features can be observed for the blue-detuning case with $\Delta_a \approx \kappa$ with phases at $\theta/\pi \approx 0.35$. This proves that the OPA pump phase has an important role in achieving strong photon antibunching.

B. Effects of pure dephasing

Pure dephasing is a source of unwanted decoherences in the system and it might affect the PB characteristics [41]. Therefore we analyze the effect of pure dephasing on the antibunching properties of the cavity photons. The effects of pure dephasing can be modeled by solving the master equation after adding another Lindblad term of the form $L_p(\rho) = \frac{\gamma_p}{2}[2a^\dagger \rho a^\dagger a - (a^\dagger a)^2 \rho - \rho (a^\dagger a)^2]$, in the master equation, where γ_p is the pure dephasing rate for the cavity mode. Figures 6(a)–6(d) show the second-order correlation function $g^{(2)}(0)$ for different pure-dephasing rates with different sets of optimized values: $G/\kappa = 8.94 \times 10^{-5}$, $\theta/\pi = -0.352$ in (a), $G/\kappa = 4.85 \times 10^{-5}$, $\theta/\pi = -0.422$ in (b), $G/\kappa = 8.94 \times 10^{-5}$, $\theta/\pi = 0.352$ in (c), and $G/\kappa = 4.85 \times 10^{-5}$, $\theta/\pi = 0.422$ in (d). It can be seen that the $g^{(2)}(0)$ still maintains the red-blue detuning asymmetry. In Fig. 6(a), for a typical pure dephasing rate of 0.01κ , the value of $\log_{10} g^{(2)}(0)$ at the red detuning with $\Delta_a \approx \kappa$ is -1.5 . With an increase in the pure-dephasing rate, $g^{(2)}(0)$ increases near the red detuning

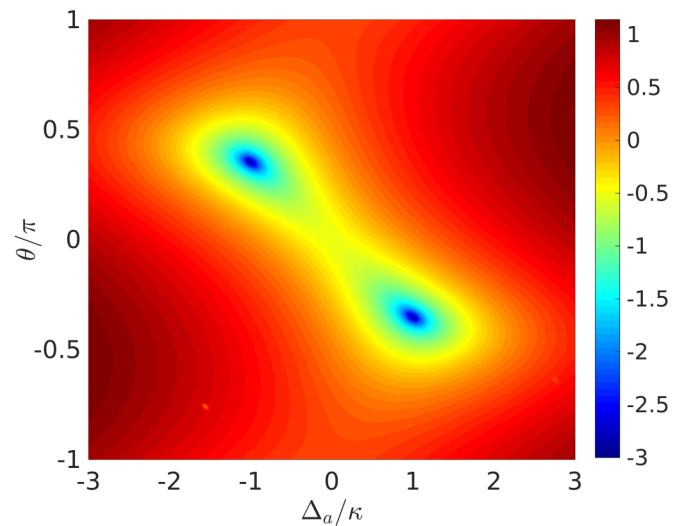


FIG. 5. Numerical results for $g^{(2)}(0)$ as a function of normalized detuning Δ_a/κ and θ/π . Other parameters are $\Omega/\kappa = 0.01$ and $G/\kappa = 8.94 \times 10^{-5}$.

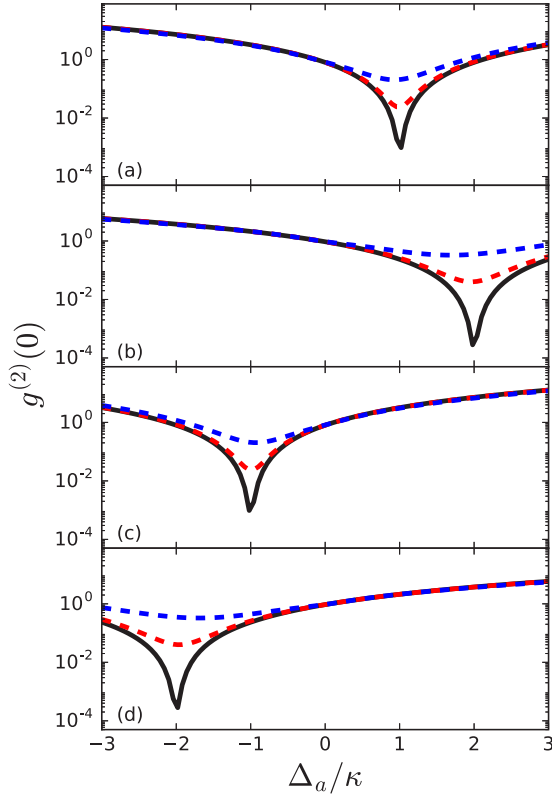


FIG. 6. $g^{(2)}(0)$ for different pure-dephasing rates. The black solid line is for the $\gamma_p = 0$ case, i.e., without any pure dephasing. The red and blue dashed lines are for $\gamma_p = 0.01\kappa$ and 0.1κ , respectively. The OPA parameters are $G/\kappa = 8.94 \times 10^{-5}$, $\theta/\pi = -0.352$ in (a), $G/\kappa = 4.85 \times 10^{-5}$, $\theta/\pi = -0.422$ in (b), $G/\kappa = 8.94 \times 10^{-5}$, $\theta/\pi = 0.352$ in (c), and $G/\kappa = 4.85 \times 10^{-5}$, $\theta/\pi = 0.422$ in (d).

at $\Delta_a \approx \kappa$. A similar feature is shown in Figs. 6(b)–6(d) for $\Delta_a \approx 2\kappa$, $-\kappa$, and -2κ , respectively. For higher values of pure-dephasing rates, $g^{(2)}(0)$ approaches classical Poissonian statistics similar to a thermal source.

IV. CONCLUSION

In conclusion, we have proposed a model to realize a strong UPB by placing an OPA medium inside a Fabry-Perot cavity under weak pump driving with $G \ll \omega_a$. We studied the photon correlations in terms of the second-order correlation function. Using analytical calculations, we derive the conditions for optimized photon antibunching in terms of the OPA pump phase θ and the OPA gain G . We find that the optimal parameters depend on the cavity-light detuning. Under the optimal parameters, the system can be used to generate sub-Poissonian light. A red-blue detuning asymmetry for pump phase θ has been observed. We find that the analytical

expressions are consistent with the numerical simulations. Also after including the pure-dephasing induced losses in the system, PB is still observed to be robust. We hope that the proposed scheme will provide us with a way to control the PB exactly and can be used as a single-photon source on-demand.

ACKNOWLEDGMENTS

The authors are grateful to Prof. G. S. Agarwal for a fruitful discussion. B.S. gratefully acknowledges support by a research fellowship from Ministry of Human Resource Development (MHRD), Government of India.

APPENDIX: INTRACAVITY STATE

The master equation for the density operator for the system considered in this work is given by

$$\dot{\rho} = i[\rho, H] + L_a(\rho), \quad (\text{A1})$$

where

$$H = \Delta_a a^\dagger a + iG(e^{i\theta} a^{\dagger 2} - e^{-i\theta} a^2) + \Omega(a^\dagger + a), \quad (\text{A2})$$

and $L_a(\rho) = \frac{\kappa}{2}(2a\rho a^\dagger - a^\dagger a\rho - \rho a^\dagger a)$ is the Liouvillian operator for the optical mode. Eq. (A1) with $G = 0$ can be solved exactly with a dynamic symmetry method as described in [44]. Following Ref. [44], one can show that if the initial intracavity state is a coherent one (i.e., $|\alpha\rangle$), then it remains a coherent state: $\rho(t) = |(\alpha + \beta)e^{(\Delta_a - i\omega)t}\rangle\langle(\alpha + \beta)e^{(\Delta_a - i\omega)t}|$, where $\Delta'_a = -i\Delta_a - \kappa/2$ and $\beta = \frac{i\Omega}{\Delta'_a}(1 - e^{-\Delta'_a t})$. In the steady state the density operator evolves into a pure coherent state: $\rho^s = |\frac{i\Omega}{\Delta'_a}e^{-i\omega t}\rangle\langle\frac{i\Omega}{\Delta'_a}e^{-i\omega t}|$. However, when $G \neq 0$, the group theoretical approach to solve the master equation becomes extremely tedious and may not be the right solution approach. As prescribed in [45], it can be shown in a straightforward way that due to the presence of the OPA, an initial coherent state evolves toward an amplitude squeezed state or a squeezed number state. This could also be seen by applying the following transformation to Eq. (A2) with $\Omega = 0$ [46]:

$$a = b \cosh r + b^\dagger e^{-i\phi} \sinh r. \quad (\text{A3})$$

By direct substitution and after some algebra one can obtain

$$H = \Lambda b^\dagger b + \sigma, \quad (\text{A4})$$

where $\Lambda = \sqrt{\Delta_a^2 - 4|G|^2}$, $r = \frac{1}{4} \ln \frac{\Delta_a - 2\sqrt{|G|^2}}{\Delta_a + 2\sqrt{|G|^2}}$, $\phi = i \ln \sqrt{-e^{2i\theta}}$, and $\sigma = (\Lambda - \Delta_a)/2$. This can also be obtained by enforcing the eigenvalue equation $H[S(\xi)|n_a\rangle] = E_{n_a}[S(\xi)|n_a\rangle]$, where $S(\xi) = e^{\xi(e^{i\theta} a^{\dagger 2} - e^{-i\theta} a^2)}$ is the squeezing operator [47]. This shows that the eigenvalue equation is satisfied if $\xi = \frac{1}{2} \tanh^{-1}(\frac{2G}{\Delta_a})$ and the eigenvalues are given by $E_{n_a} = \Delta_a(n_a \cosh 2\xi + \sinh^2 \xi) - G(2n_a + 1) \sinh 2\xi$.

- [1] A. Imamoglu, H. Schmidt, G. Woods, and M. Deutsch, *Phys. Rev. Lett.* **79**, 1467 (1997).
 [2] M. J. Hartmann, F. G. S. L. Brandao, and M. B. Plenio, *Nat. Phys.* **2**, 849 (2006).

- [3] A. D. Greentree, C. Tahan, J. H. Cole, and L. C. L. Hollenberg, *Nat. Phys.* **2**, 856 (2006).
 [4] D. G. Angelakis, M. F. Santos, and S. Bose, *Phys. Rev. A* **76**, 031805 (2007).

- [5] D. E. Chang, V. Gritsev, G. Morigi, V. Vuletić, M. D. Lukin, and E. A. Demler, *Nat. Phys.* **4**, 884 (2008).
- [6] A. Miranowicz, J. Bajer, M. Paprzycka, Y.-x. Liu, A. M. Zagoskin, and F. Nori, *Phys. Rev. A* **90**, 033831 (2014).
- [7] P. Rabl, *Phys. Rev. Lett.* **107**, 063601 (2011).
- [8] P. Komar, S. D. Bennett, K. Stannigel, S. J. M. Habraken, P. Rabl, P. Zoller, and M. D. Lukin, *Phys. Rev. A* **87**, 013839 (2013).
- [9] J.-Q. Liao and F. Nori, *Phys. Rev. A* **88**, 023853 (2013).
- [10] H. Wang, X. Gu, Y.-x. Liu, A. Miranowicz, and F. Nori, *Phys. Rev. A* **92**, 033806 (2015).
- [11] Y.-x. Liu, X.-W. Xu, A. Miranowicz, and F. Nori, *Phys. Rev. A* **89**, 043818 (2014).
- [12] A. Miranowicz, M. Paprzycka, Y.-x. Liu, J. Bajer, and F. Nori, *Phys. Rev. A* **87**, 023809 (2013).
- [13] G. H. Hovsepyan, A. R. Shahinyan, and G. Y. Kryuchkian, *Phys. Rev. A* **90**, 013839 (2014).
- [14] W.-W. Deng, G.-X. Li, and H. Qin, *Phys. Rev. A* **91**, 043831 (2015).
- [15] Y.-x. Liu, A. Miranowicz, Y. B. Gao, J. Bajer, C. P. Sun, and F. Nori, *Phys. Rev. A* **82**, 032101 (2010).
- [16] N. Didier, S. Pugnetti, Y. M. Blanter, and R. Fazio, *Phys. Rev. B* **84**, 054503 (2011).
- [17] A. Miranowicz, J. Bajer, N. Lambert, Y.-x. Liu, and F. Nori, *Phys. Rev. A* **93**, 013808 (2016).
- [18] K. M. Birnbaum, A. Boca, R. Miller, A. D. Boozer, T. E. Northup, and H. J. Kimble, *Nature (London)* **436**, 87 (2005).
- [19] B. Dayan, A. S. Parkins, T. Aoki, E. P. Ostby, K. J. Vahala, and H. J. Kimble, *Science* **319**, 1062 (2008).
- [20] A. Faraon, I. Fushman, D. Englund, N. Stoltz, P. Petroff, and J. Vučković, *Nat. Phys.* **4**, 859 (2008).
- [21] C. Lang, D. Bozyigit, C. Eichler, L. Steffen, J. M. Fink, A. A. Abdumalikov, Jr., M. Baur, S. Filipp, M. P. daSilva, A. Blais, and A. Wallraff, *Phys. Rev. Lett.* **106**, 243601 (2011).
- [22] A. J. Hoffman, S. J. Srinivasan, S. Schmidt, L. Spietz, J. Aumentado, H. E. Türeci, and A. A. Houck, *Phys. Rev. Lett.* **107**, 053602 (2011).
- [23] D. Gerace, H. E. Türeci, A. Imamoglu, V. Giovannetti, and R. Fazio, *Nat. Phys.* **5**, 281 (2009).
- [24] I. Carusotto, D. Gerace, H. E. Türeci, S. De Liberato, C. Ciuti, and A. Imamoglu, *Phys. Rev. Lett.* **103**, 033601 (2009).
- [25] M. J. Hartmann, *Phys. Rev. Lett.* **104**, 113601 (2010).
- [26] T. C. H. Liew and V. Savona, *Phys. Rev. Lett.* **104**, 183601 (2010).
- [27] J. Tang, W. Geng, and X. Xu, *Sci. Rep.* **5**, 9252 (2015).
- [28] A. Majumdar, M. Bajcsy, A. Rundquist, and J. Vučković, *Phys. Rev. Lett.* **108**, 183601 (2012).
- [29] W. Zhang, Z. Yu, Y. Liu, and Y. Peng, *Phys. Rev. A* **89**, 043832 (2014).
- [30] X.-W. Xu and Y. Li, *Phys. Rev. A* **90**, 033809 (2014).
- [31] M. Bamba, A. Imamoglu, I. Carusotto, and C. Ciuti, *Phys. Rev. A* **83**, 021802 (2011).
- [32] H. Z. Shen, Y. H. Zhou, H. D. Liu, G. C. Wang, and X. X. Yi, *Opt. Express* **23**, 32835 (2015).
- [33] S. Ferretti, V. Savona, and D. Gerace, *New J. Phys.* **15**, 025012 (2013).
- [34] H. Flayac, D. Gerace, and V. Savona, *Sci. Rep.* **5**, 11223 (2015).
- [35] H. Z. Shen, Y. H. Zhou, and X. X. Yi, *Phys. Rev. A* **91**, 063808 (2015).
- [36] H. Flayac and V. Savona, *Phys. Rev. A* **94**, 013815 (2016).
- [37] D. Gerace and V. Savona, *Phys. Rev. A* **89**, 031803 (2014).
- [38] Y. H. Zhou, H. Z. Shen, and X. X. Yi, *Phys. Rev. A* **92**, 023838 (2015).
- [39] M.-A. Lemonde, N. Didier, and A. A. Clerk, *Phys. Rev. A* **90**, 063824 (2014).
- [40] X.-W. Xu and Y.-J. Li, *J. Phys. B* **46**, 035502 (2013).
- [41] V. Savona, [arXiv:1302.5937v2](https://arxiv.org/abs/1302.5937v2).
- [42] P. D. Nation, J. R. Johansson, M. P. Blencowe, and F. Nori, *Rev. Mod. Phys.* **84**, 1 (2012).
- [43] P. Knight and G. Gerry, *Introductory Quantum Optics* (Cambridge University Press, Cambridge, UK, 2005).
- [44] A. B. Klimov and S. M. Chumakov, *A Group-Theoretical Approach to Quantum Optics* (Wiley, New York, 2009).
- [45] D. F. Walls and G. J. Milburn, *Quantum Optics* (Springer, New York, 2007).
- [46] G. S. Agarwal, *Quantum Optics* (Cambridge University Press, Cambridge, UK, 2013).
- [47] M. Bhattacharya, H. Shi, and S. Preble, *Am. J. Phys.* **81**, 267 (2013).